

pubs.acs.org/JACS Article

# Two-State Hydrogen Atom Transfer Reactivity of Unsymmetric [Cu<sub>2</sub>(O)(NO)]<sup>2+</sup> Complexes

Samantha Carter, Wenjie Tao, Rajat Majumder, Alexander Yu. Sokolov,\* and Shiyu Zhang\*



Cite This: J. Am. Chem. Soc. 2023, 145, 17779–17785



**Read Online** 

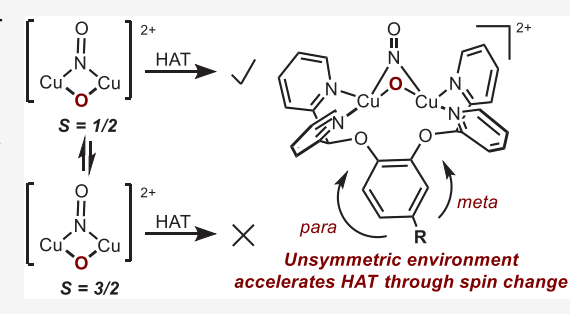
**ACCESS** I

III Metrics & More

Article Recommendations

s Supporting Information

**ABSTRACT:** We report the temperature-dependent spin switching of dicopper oxo nitrosyl  $[Cu_2(O)(NO)]^{2+}$  complexes and their influence on hydrogen atom transfer (HAT) reactivity. Electron paramagnetic resonance (EPR) and Evans method analysis suggest that  $[Cu_2(O)(NO)]^{2+}$  complexes transition from the S=1/2 to the S=3/2 state around ca. 202 K. At low temperatures (198 K) where S=3/2 dominates, a strong correlation between the rate of HAT  $(k_{\text{HAT}})$  and the population of the S=1/2 state was identified  $(R^2=0.988)$ , suggesting that the HAT by  $[Cu_2(O)(NO)]^{2+}$  complexes proceeds by the S=1/2 isomer. Installation of functional groups that introduce an unsymmetric secondary coordination environment accelerates the HAT rates through perturbation of the spin equilibria.



Given the often unsymmetric coordination sphere of bimetallic active sites in natural proteins, we anticipate that similar strategies could be employed by metalloenzymes to control HAT reactions.

### INTRODUCTION

Metalloenzymes utilize high-energy metal oxo species to cleave strong aliphatic C–H bonds with high fidelity. Understanding the key features that impact the metal oxo's hydrogen atom transfer (HAT) reactivity could inform the design of synthetic catalysts that mimic nature's enzymes. A controversial theory that explains the metal oxo's HAT reactivity is the two-state reactivity model. This model suggests that metal oxo species can undergo spin-crossing along the reaction coordinates from reactants to products (Figure 1A). The origin of the two-state HAT reactivity was traced to the fact that  $\text{Fe}^{\text{IV}}$ =O,  $^{9-13}$   $\text{Mn}^{\text{V}}$ =O,  $^{14-16}$  and  $\text{Cr}^{\text{V}}$ = $\text{O}^{17}$  species have a dense manifold of spin states with very close energies. Some of these spin states can provide particularly low energy paths for otherwise difficult HAT processes under one-state scenarios (Figure 1A).

Despite the popular use of the two-state reactivity model in explaining the reactivity pattern of bond activation, experimentally probing two-state oxidative reactivity remains difficult. This is mainly due to the challenges associated with isolating the highly reactive metal oxo species at two different spin states. To provide evidence for the two-state reactivity of metal oxo species, one approach involves systematically varying the electronic properties of substrates and comparing rates of HAT and oxygen atom transfer (OAT). If HAT and OAT occur on two different spin states, then opposite trends in their rates are expected. Nonetheless, clear examples of two-state HAT reactivity, where the barriers of HAT fluctuate at different spin states (Figure 1A), remain rare.

Only a limited number of systematic studies have been conducted on HAT by geometrically analogous metal oxo complexes at different spin states.  $^{6,22,23}$  Nam et al. investigated the HAT reactivity of a series of non-heme iron(IV) oxo species and found that the S=2 species abstracts H atoms faster than the S=1 species.  $^{23-25}$  However, Kojima and Que have reported Ru oxo and Fe oxo species that exhibit similar HAT rates at different spin states. Seminal work by Que et al. showed that an open-core high-spin  $[Fe^{III}-O-Fe^{IV}=O]^{3+}$  species oxidizes hydrocarbons 6 orders of magnitude faster than the diamond-core low-spin delocalized  $[Fe^{3.5}(\mu-O)_2Fe^{3.5}]^{3+}$  analog (Figure 1B). The spin state change from S=1 to S=2 was considered to be a potential contributor to the drastically different HAT reactivity. Recently, Wang et al. reported HAT rate enhancements of similar magnitude with an open-core  $[Co^{III}-O-Co^{IV}=O]^{3+}$  species; but no spin state change was observed in this case.

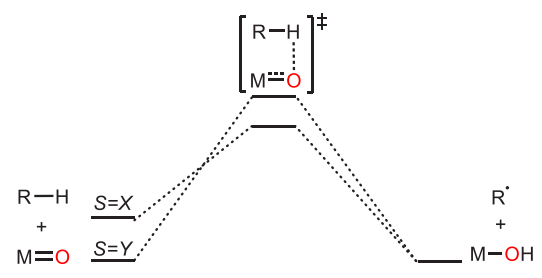
A common limitation of these studies is that the metal oxo complexes being compared in each case have either different coordination environments or charges, making it difficult to attribute the HAT rate enhancement to the change in spin state alone. Herein, we report the two-state HAT reactivity of a series of dicopper oxo nitrosyl  $[Cu_2(O)(NO)]^{2+}$  complexes.

Received: May 1, 2023 Published: August 4, 2023





A. Energy profile of a two-state HAT reaction by M=O



B. Spin state influences HAT reactivity of diFe oxo complexes

$$\begin{bmatrix} 3.5 & 0 & 3.5 \\ Fe & 0 & Fe \end{bmatrix}$$

$$\begin{array}{c} 3.5 & 0 & 3.5 \\ Fe & 0 & 0 & 1 \\ Charge & Charge \\ delocalization & Charge \\ delocalization & S = 1 & S = 2 \\ \hline \times 10^6 & HAT \ rate \ enhancement & Charge \\ Charge & Cha$$

C. This work: Two-spin HAT reactivity of [Cu<sub>2</sub>(O)(NO)]<sup>2+</sup> complexes

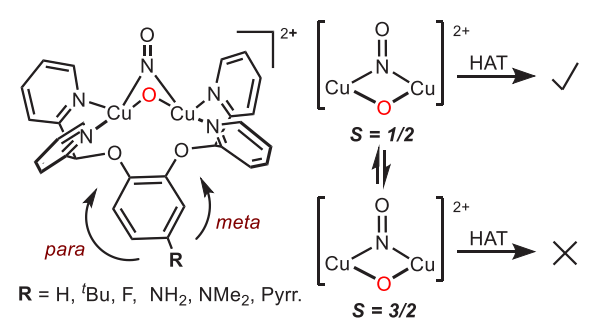


**Figure 1.** (A) Influence of two spin states on HAT barriers  $(X \neq Y)$ . (B) Comparison of HAT reactivity of open and closed core diiron oxo species reported by Que et al. 26 (C) Spin switching of [RLCu<sub>2</sub>(O)-(NO)]<sup>2+</sup> from S = 3/2 to S = 1/2 state, which is more reactive toward HAT.

Spectroscopic analysis revealed that [Cu<sub>2</sub>(O)(NO)]<sup>2+</sup> complexes exist in the S = 1/2 state at high temperature and the S = 3/2 state at low temperature (Figure 1C). The mechanism of HAT by  $[Cu_2(O)(NO)]^{2+}$  is consistent with a two-state reactivity model illustrated in Figure 1A. Despite the S = 3/2being more stable, the HAT reaction occurs through a fast preequilibrium between the S = 3/2 and S = 1/2 states, followed by a rate-limiting HAT step on the S = 1/2 surface. Perturbation of the symmetry in the secondary coordination environment was found to shift the spin equilibrium, which influences the HAT reactivity. As unsymmetric environments are prevalent in metalloenzymes, our study suggests that even minor changes in the secondary coordination sphere can alter the spin population of metal oxo species. This could be a strategy leveraged by nature to control the HAT rates.

#### RESULTS AND DISCUSSION

Spin Switching of Dicopper Oxo Nitrosyl Species. In our previous studies, we prepared the symmetric [HLCu<sub>2</sub>(O)-(NO)]<sup>2+</sup> species (Figure 1C) by activating nitrite or NO at the dicopper center. <sup>28,29</sup> This complex exhibits HAT, C-H hydroxylation, and S-nitrosation reactivity. We initially assigned  $[^{H}LCu_{2}(O)(NO)]^{2+}$  as an S = 1/2 species based on the S = 1/2 EPR signal around 300 mT and the N=O<sup>-</sup> stretch at 1554 cm<sup>-1</sup>. However, a recent computational study by

Yoshizawa and Shiota proposed an alternative S = 3/2 state for the  $[^{H}LCu_{2}(O)(NO)]^{2+}$  complex.<sup>3</sup>

Encouraged by their work, we further examined the EPR of  $[^{H}LCu_{2}(O)(NO)]^{2+}$  at low temperature (5 K) and high microwave power (2.0 mW) and observed an S = 3/2 signal at g = 1.95. Spectral simulation of the S = 3/2 signal allowed us to determine zero-field splitting parameters of  $D = 0.2 \text{ cm}^{-1}$  and E/D = 0.3 (Figure 2, red). Temperature-dependent EPR

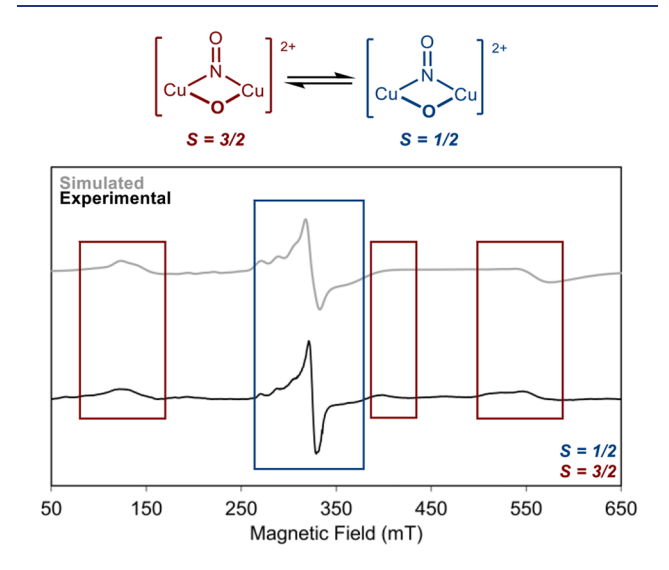


Figure 2. Simulated (gray) and experimental (black) EPR spectra of  $[^{H}LCu_{2}(O)(NO)]^{2+}$  at 5 K with high microwave power (2.0 mW). Both the S = 1/2 signal (blue,  $g_x = 1.76$ ,  $g_y = 2.09$ ,  $g_z = 2.28$ ,  $A_z = 550$ , weight = 44%) and the S = 3/2 signal (red,  $g_{iso} = 1.95$ , D = 0.2 cm<sup>-1</sup>, E/D = 0.3, weight = 56%) are observed.

saturation studies from 5 to 25 K (see the Supporting Information, Figures S66-S69) suggest that the spin-switching behavior is best explained by valence isomerism, <sup>33,34</sup> where the S = 1/2 and S = 3/2 states have different valence arrangement due to reversible electron transfers between Cu ions and the redox-active nitrosyl ligand. Valence isomerization is often observed when the energy levels of the ligand frontier orbitals lie close to the valence electrons of the metal ions. Copper nitrosyl complexes are expected to satisfy these criteria.

We next investigated the spin state of [HLCu<sub>2</sub>(O)(NO)]<sup>2+</sup> in solution as a function of temperature by performing a series of Evans method studies (Figure 3).36 A solution of

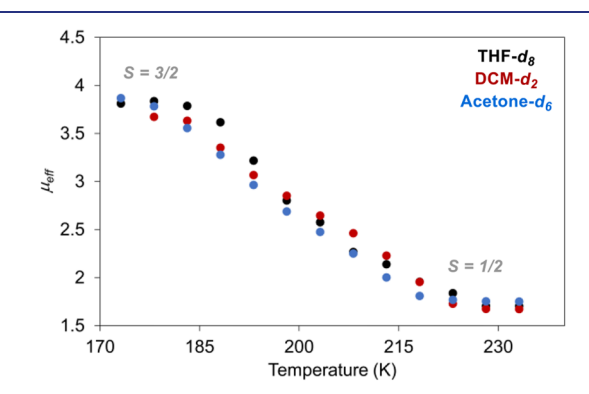


Figure 3.  $\mu_{\text{eff}}$  versus temperature (K) plot for  $[^{\text{H}}LCu_2(O)(NO)]^{2+}$ determined by the solution Evans method study in acetone- $d_6$  (blue), THF- $d_8$  (black), and DCM- $d_2$  (red).

 $[^{\rm H}{\rm LCu_2(O)(NO)}]^{2+}$  in acetone- $d_6$  (blue) exhibits a  $\mu_{\rm eff}$  of 1.75 ( $\chi_{\rm M}T=0.44~{\rm cm}^3~{\rm K~mol}^{-1}$ ) at 233 K, consistent with an S=1/2 spin state (expected  $\mu_{\rm eff}=1.73$ ). However, when the temperature is decreased to 173 K, the  $[^{\rm H}{\rm LCu_2(O)(NO)}]^{2+}$  complex undergoes spin switching to the S=3/2 state, as evidenced by the observed  $\mu_{\rm eff}$  of 3.87 (expected  $\mu_{\rm eff}=3.87$ ). Importantly, similar spin-transition behaviors were observed in both THF- $d_8$  (black) and DCM- $d_2$  (red), suggesting that the spin transition is not due to the coordination of solvent molecules.

CASSCF Calculations of S = 1/2 and S = 3/2 States. The approximately 1:1 distribution of S = 1/2 and S = 3/2 state determined by the Evans method and EPR studies contradicts the previous density functional theory (DFT) study by Yoshizawa and Shiota (B3LYP/6-311G\*\*), which suggests the S = 1/2 state is more stable than the S = 3/2 state by 28 kcal/mol.<sup>32</sup> Accurate DFT calculation of spin-state splitting is challenging, and the results are highly sensitive to the nature of the functionals.<sup>37–39</sup> To address this issue, we performed state-averaged CASSCF calculations on the crystal structure of  $[^{\rm H}LCu_2({\rm O})({\rm NO})]^{2+}$  using a [13e, 15o] active space (see Supporting Information for details). To account for significant dynamical correlation in such systems, we performed strongly contracted N-electron valence perturbation theory (SC-NEVPT2) calculations on top of CASSCF.<sup>40</sup>

The calculation reveals a doublet/quartet splitting of 0.16 kcal/mol with a def2-SVP basis set and 12 kcal/mol with a def2-TZVP basis set. These doublet/quartet splitting energies are much smaller compared to those predicted by DFT. However, they are still higher than the experimental values, perhaps due to the solid-state or solution environment of the  $[^{\rm H}L{\rm Cu}_2({\rm O})({\rm NO})]^{2+}$  structure, zero-point vibrational effects, and approximations in the SC-NEVPT2/SA-CASSCF method. Analysis of the SA-CASSCF spin density for the S=1/2 and S=3/2 states shows that the unpaired electron is localized on the bridging oxo ligand (Figure 4).

Synthesis of Unsymmetric Dicopper Oxo Nitrosyl Complexes. Local magnetic and electric fields are known to influence the relative energies of different spin states. Therefore, we hypothesize that modification of the secondary coordination environment may shift the spin equilibria of  $[^RLCu_2(O)(NO)]^{2+}$  complexes. To test this hypothesis, we introduced substituents (R) with different electronic properties at the 4-position of the catechol linker (Scheme 1) to perturb the symmetric environment of the  $[Cu_2(O)(NO)]^{2+}$  complexes. We selected five  $[^RLCu_2(O)(NO)]^{2+}$  derivatives (R =  $^tBu$ , F, NH<sub>2</sub>, NMe<sub>2</sub>, and pyrrolidinyl (Pyrr)) that can be isolated as pure microcrystalline materials for magnetism and reactivity studies.

The unsymmetric ligands (<sup>R</sup>L) were synthesized and utilized to prepare the corresponding dicopper complexes [<sup>R</sup>LCu<sup>I</sup><sub>2</sub>(MeCN)<sub>2</sub>]BAr<sup>F</sup><sub>2</sub> (BAr<sup>F</sup> = tetrakis(3,5-bis-(trifluoromethyl)phenyl)borate). <sup>1</sup>H and <sup>13</sup>C NMR characterization and elemental analysis support the formation of dicopper(I,I) acetonitrile complexes. (See Supporting Information.) Cyclic voltammetry of the new dicopper(I,I) complexes in MeCN with 0.1 M TBAClO<sub>4</sub> electrolyte shows that the quasi-reversible redox couples of Cu<sup>II</sup>Cu<sup>I</sup>/Cu<sup>I</sup>Cu<sup>I</sup> are located within a ±36 mV window of the parent [<sup>H</sup>LCu<sup>I</sup><sub>2</sub>(MeCN)<sub>2</sub>]<sup>2+</sup> complex, indicating that altering R has minimal effects on the redox properties of the dicopper core. This result is consistent with the weakly coordinating nature of

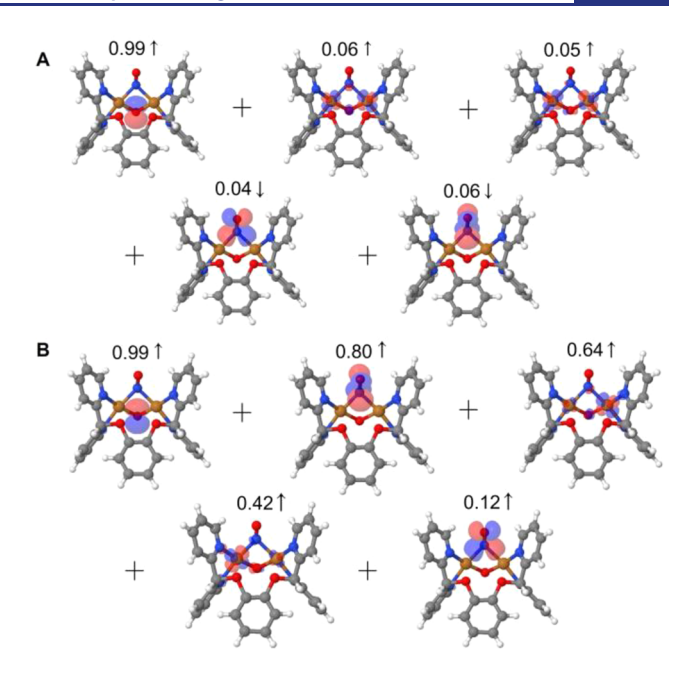


**Figure 4.** Analysis of  $[^{H}LCu_{2}(O)(NO)]^{2+}$  spin density for the (A) S=1/2 and (B) S=3/2 states computed using SA-CASSCF (13e, 15o) with the def2-TZVP basis set. The numbers next to each orbital plot indicate eigenvalues of spin density; arrows denote spin projection.

# Scheme 1. Synthesis of Unsymmetric $[^{R}LCu_{2}(O)(NO)]^{2+}$

the catechol linker to the Cu center (average Cu–O distance 2.757 Å in  $[{}^HLCu_2(O)(NO)]^{2+}).^{28}$ 

Treatment of  $[^{R}LCu_{2}^{1}(MeCN)_{2}]^{2+}$  species with four equivalents of NO in acetone at 233 K resulted in the formation of red  $[^{R}LCu_{2}(O)(NO)]^{2+}$  complexes, as evidenced by the increase in the UV–vis features at 525 nm ( $\varepsilon \approx 2500 \, \mathrm{M}^{-1} \, \mathrm{cm}^{-1}$ ). EPR studies demonstrated that all of the  $[^{R}LCu_{2}(O)(NO)]^{2+}$  complexes coexist in S = 1/2 and S = 3/2 states. These new  $[^{R}LCu_{2}(O)(NO)]^{2+}$  complexes are stable at 233 K and can be isolated as microcrystalline materials from 49% to 68% yields.

An Evans method study was performed on the five unsymmetric  $[^{\mathbf{R}}\mathbf{L}\mathbf{C}\mathbf{u}_{2}(\mathbf{O})(\mathbf{N}\mathbf{O})]^{2+}$  complexes. We found that the spin transition temperature  $(T_{1/2})$  from the S=1/2 to the S=3/2 spin state varies significantly based on the  $\mathbf{R}$  group on the catechol linker (Figure 5). The data were fitted with a

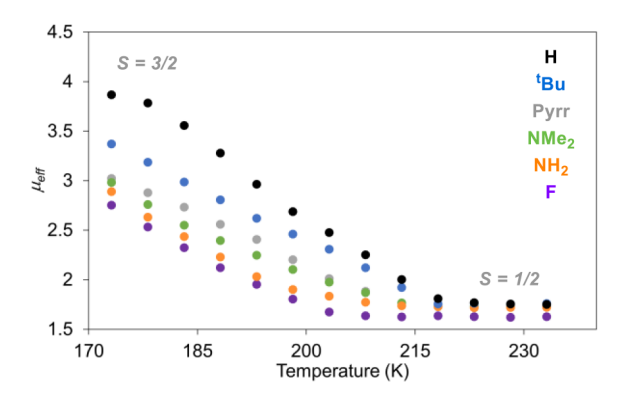


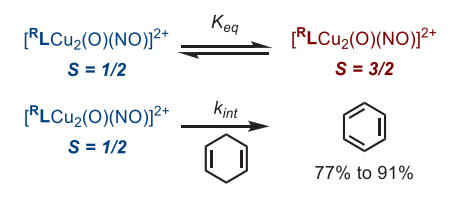
**Figure 5.** Plots of  $\mu_{\text{eff}}$  determined by variable-temperature Evans method studies for  $[^{R}LCu_{2}(O)(NO)]^{2+}$  where R = H (black),  $^{t}Bu$  (blue), Pyrr (gray), NMe<sub>2</sub> (green), NH<sub>2</sub> (orange), and F (purple).

standard solution spin transition model (see Supporting Information). The symmetric [ $^{\rm H}L{\rm Cu}_2({\rm O})({\rm NO})$ ] $^{2+}$  has the highest transition temperature  $T_{1/2}$  of 202 K, while the  $T_{1/2}$  decreases to 188, 180, 177, 175, and 173 K for  ${\bf R}={}^t{\rm Bu}$ , Pyrr, NMe<sub>2</sub>, NH<sub>2</sub>, and F, respectively (Table 1). This finding shows that the distribution between the S=1/2 and S=3/2 isomers is sensitive to the secondary coordination environment of the  $[{\rm Cu}_2({\rm O})({\rm NO})]^{2+}$  core. An unsymmetric environment appears to induce a decrease in  $T_{1/2}$ , regardless of whether the substituent is electron donating or withdrawing.

HAT Reactivity of Dicopper Complexes. The  $[^{R}LCu_{2}(O)(NO)]^{2+}$  series allows us to investigate how the spin distributions of S=1/2 and S=3/2 impact HAT reactivity. Specifically, we monitored the reaction between  $[^{R}LCu_{2}(O)(NO)]^{2+}$  and the hydrogen atom donor 1,4-cyclohexadiene (Scheme 2).  ${}^{1}H$  NMR analysis of the reaction mixture of  $[^{R}LCu_{2}(O)(NO)]^{2+}$  and cyclohexadiene showed that all of the  $[^{R}LCu_{2}(O)(NO)]^{2+}$  complexes oxidize cyclohexadiene to benzene in high yields (77–91%). Second-order HAT rate constants ( $k_{\rm HAT}$ ) were determined using UV–vis spectroscopy under pseudo-first-order conditions with an excess amount of C–H substrate at 198 K (see the Supporting Information, Table 1).

Interestingly, the HAT rates of the  $[^{R}LCu_{2}(O)(NO)]^{2+}$  complexes do not follow any trend predicted by the Hammett parameters (Figure 6A,B). Plots of  $\ln(k_{\rm HAT})$  versus  $\sigma_{\rm para}$  or  $\sigma_{\rm meta}$  show weak correlations ( $R^{2}=0.16$  and 0.0016), and we did not observe a V-shaped Hammett plot that would suggest a change in the reaction mechanism. Previous studies by Karlin suggested that electron-rich dicopper bis- $\mu$ -oxo/peroxo species abstract H atoms faster compared to electron-poor ones. Hat rates do not correlate with the redox potentials of dicopper (I,I) complexes either. Surprisingly, the two most reactive species, R = F and  $NH_{2}$ , contain opposing electronics, and the symmetric  $[^{H}LCu_{2}(O)(NO)]^{2+}$  exhibits the slowest

Scheme 2. HAT Reactivity of  $[Cu_2(O)(NO)]^{2+}$  Complexes



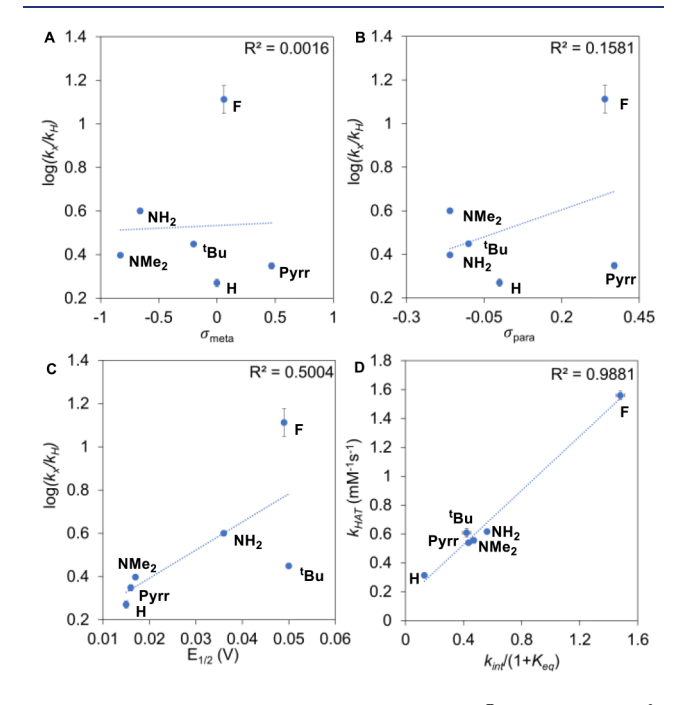


**Figure 6.** Plots of the logarithm of HAT rates by  $[^{R}LCu_{2}(O)(NO)]^{2+}$  where R = H,  $^{t}Bu$ , Pyrr, NMe<sub>2</sub>, NH<sub>2</sub>, and F vs (A)  $\sigma_{meta}$ , (B)  $\sigma_{para}$ , (C)  $E_{1/2}$  potential of dicopper(I,I) precursors, and (D) the  $k_{HAT}$  (mM<sup>-1</sup> s<sup>-1</sup>) vs the  $k_{int}$ /(1 +  $K_{eq}$ ) at 198 K.

HAT rate. Besides Hammett parameters, we attempted to determine the O–H BDFE values of  $[^{R}LCu_{2}(O)(NO)]^{2+}$ , as they are valuable in understanding the trend of HAT rates. However, due to the instability of  $[Cu_{2}(OH)(NO)]^{2+}$  species, we could not measure the  $pK_{a}$  value of the O–H moiety reliably.

In considering an alternative interpretation for the trend of the HAT rate, we hypothesize that one spin state of  $[Cu_2(O)(NO)]^{2+}$  species is more reactive toward HAT than the other. At the temperature the HAT rates were measured (198 K), the S=3/2 state of  $[Cu_2(O)(NO)]^{2+}$  complexes is more stable (Figure 5), and they must access the HAT-active S=1/2 state through a spin transition (Figure 7). Based on this proposed mechanism, the spin population of S=1/2 versus S=3/2 influences HAT rates as a pre-equilibrium step with the following rate law expression (see Supporting Information):<sup>39</sup>

Table 1. Characterization of the [RLCu<sub>2</sub>(O)(NO)]<sup>2+</sup> Complexes

R	Н	Pyrr	$NMe_2$	<sup>t</sup> Bu	$\mathrm{NH}_2$	F
$E_{1/2}$ (mV)	15	17	51	50	36	49
$T_{1/2}$ (K)	202	188	180	177	175	173
$K_{ m eq}$	1.41	0.241	0.183	0.444	0.0974	0.0540
$k_{ m HAT}~({ m mM}^{-1}~{ m s}^{-1})$	0.27(2)	0.35(1)	0.40(1)	0.45(0)	0.60(1)	1.11(7)
$k_{\rm int}~({ m mM}^{-1}~{ m s}^{-1})$	3.12(1)	5.22(1)	5.66(2)	6.08(3)	6.14(1)	15.6(3)

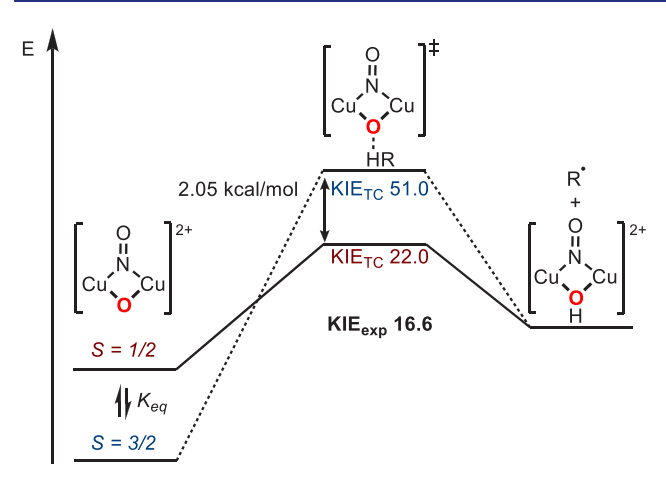


**Figure 7.** Energy profile for the HAT reaction of  $[Cu_2(O)(NO)]^{2+}$  species with the computed  $KIE_{TC}$  for S=1/2 and S=3/2. The experimental  $KIE_{exp}$  (16.6) is consistent with S=1/2 being the more reactive HAT state.

$$k_{\rm HAT} = k_{\rm int}/(1 + K_{\rm eq}) \tag{1}$$

$$K_{\text{eq}} = \left[ \text{Quartet/Doublet} \right]$$
 (2)

where  $k_{\rm HAT}$  is the observed second-order rate constant of hydrogen atom transfer.  $K_{\rm eq}$  is the equilibrium constant between the S=3/2 state and S=1/2 state, and it can be calculated with  $\Delta H$  and  $\Delta S$  of the spin transition at 198 K (Table 1; see Supporting Information).  $k_{\rm int}$  is the intrinsic HAT rate on the HAT-active spin surface. An approximation of the trend of  $k_{\rm int}$  as the S=1/2 isomer can be made by measuring the rate of HAT at 233 K, as the populations of S=1/2 are >95% for all  $\left[{\rm Cu_2(O)(NO)}\right]^{2+}$  derivatives at this temperature. If the HAT reaction follows the mechanism outlined in Scheme 2, then  $k_{\rm HAT}$  should exhibit a linear correlation with  $k_{\rm int}/(1+K_{\rm eq})$  according to eq 1. Indeed, we found a strong correlation between  $k_{\rm HAT}$  and  $1/(1+K_{\rm eq})$  with  $R^2=0.9881$  (Figure 6D), validating the HAT mechanism proposed in Scheme 2.

## Determination of the HAT-Active Spin State via KIE.

To provide further evidence for the two-state HAT reactivity, we set out to verify if S = 1/2 is the HAT-active state using kinetic isotope effect (KIE) experiments. Shaik et al. showed that DFT-computed KIE values could be used to identify the HAT-active spin state. 53-56 Accordingly, we performed a KIE study of HAT from 1,4-cyclohexadiene to [HLCu<sub>2</sub>(NO)(O)]<sup>2+</sup> in acetone at -40 °C. An experimental KIE of 16.6 was determined using 1,4-cyclohexadiene and cyclohexadiene-d<sub>8</sub> (Figure S46). Tunneling corrected kinetic isotope effect values (KIE<sub>TC</sub>) were computed for both S = 1/2 and S = 3/2 states using DFT at the UBP86/TZVP level with Grimme's threebody dispersion correction (D3). The calculated free energy HAT barrier at the S = 1/2 surface is ca. 2.05 kcal/mol lower than that of the S = 3/2 surface, consistent with the experimental observation that S = 1/2 is the HAT-active state (Figure 7). The KIE $_{TC}$  was then calculated using the total rate constants according to eq 3: $^{53,55-58}$ 

$$KIE_{TC} = \frac{\binom{2/4}{k(H)}}{\binom{2/4}{k(D)}}$$
(3)

where  $^{2/4}k_2(H)$  and  $^{2/4}k_2(D)^{55,59}$  are the calculated total rate constants at the spin multiplicity (2S + 1) based on the HAT

barriers (see Supporting Information eqs S12–S16). The resulting KIE<sub>TC</sub> at the doublet spin surface is 22.0, while that for the quartet surface is 51.0. Therefore, the experimental KIE of 16.6 is consistent with S = 1/2 being the more HAT-active spin state for HAT (Figure 7).

#### CONCLUSION

In summary, we reported the spin-switching behavior of  $[Cu_2(O)(NO)]^{2+}$  between S=1/2 and S=3/2 isomers and its influence on the HAT reactivity. EPR and Evans method study demonstrated that the S=1/2 and S=3/2 isomers are nearly degenerate, with S=3/2 being more stable at low temperatures. Kinetic studies, along with tunneling-corrected KIE calculations, suggest that  $[Cu_2(O)(NO)]^{2+}$  undergoes a rapid spin transition from the S=3/2 to S=1/2 state, where HAT occurs as the rate-limiting step. This mechanism is reminiscent of Mayer's report on spin-forbidden HAT from the Co(II) imidazoline complex to the phenoxyl radical  $(RO^{\bullet})$ .

The spin transition temperature and spin equilibrium are sensitive to the secondary coordination environment of the dicopper complex. Installation of a remote functional group shifts  $T_{1/2}$  from ca. 202 K in a symmetric ligand environment to ca. 173 K in an unsymmetric environment. Though it is unclear how the substituents shift the spin equilibria, spin partition clearly influences the rate of HAT in this case since the S = 1/2 state is more reactive toward HAT than the S = 3/22 state. Given the often unsymmetric coordination sphere of bimetallic active sites in natural proteins, we anticipate that similar strategies could be employed in nature to control HAT reactions in metalloenzymes. Although the rate enhancement of HAT in our case is modest, the additive effect of many unsymmetric features around bimetallic sites might result in appreciable HAT enhancements. This will be the subject of our future studies.

# ASSOCIATED CONTENT

### Supporting Information

The Supporting Information is available free of charge at https://pubs.acs.org/doi/10.1021/jacs.3c04510.

Experimental details, including characterization data, spectra, computational procedures, and results (PDF)

## AUTHOR INFORMATION

# **Corresponding Authors**

Alexander Yu. Sokolov — Department of Chemistry & Biochemistry, The Ohio State University, Columbus, Ohio 43210, United States; orcid.org/0000-0003-2637-4134; Email: sokolov.8@osu.edu

Shiyu Zhang — Department of Chemistry & Biochemistry, The Ohio State University, Columbus, Ohio 43210, United States; orcid.org/0000-0002-2536-4324; Email: zhang.8941@osu.edu

#### Authors

Samantha Carter – Department of Chemistry & Biochemistry, The Ohio State University, Columbus, Ohio 43210, United States

Wenjie Tao − Department of Chemistry & Biochemistry, The Ohio State University, Columbus, Ohio 43210, United States; orcid.org/0000-0003-3311-7793

Rajat Majumder — Department of Chemistry & Biochemistry, The Ohio State University, Columbus, Ohio 43210, United States

Complete contact information is available at: https://pubs.acs.org/10.1021/jacs.3c04510

#### **Notes**

The authors declare no competing financial interest.

#### ACKNOWLEDGMENTS

This material is based on work supported by the U.S. National Science Foundation under award no. CHE-2246440. We thank Prof. Hannah Shafaat for valuable discussions on EPR analysis of the  $[Cu_2(NO)(O)]^{2+}$  complex. R.M. and A.Y.S. were supported by the National Science Foundation under award no. CHE-2044648. Theoretical calculations were performed at the Ohio Supercomputer Center under project Nos. PAS1963 and PAS1298.

#### REFERENCES

- (1) Elwell, C. E.; Gagnon, N. L.; Neisen, B. D.; Dhar, D.; Spaeth, A. D.; Yee, G. M.; Tolman, W. B. Copper-Oxygen Complexes Revisited: Structures, Spectroscopy, and Reactivity. *Chem. Rev.* **2017**, *117*, 2059–2107.
- (2) Jasniewski, A. J.; Que, L. Dioxygen Activation by Nonheme Diiron Enzymes: Diverse Dioxygen Adducts, High-Valent Intermediates, and Related Model Complexes. *Chem. Rev.* **2018**, *118*, 2554–2592.
- (3) Saouma, C. T.; Mayer, J. M. Do Spin State and Spin Density Affect Hydrogen Atom Transfer Reactivity? *Chem. Sci.* **2014**, *5*, 21–31.
- (4) Schröder, D.; Shaik, S.; Schwarz, H. Two-State Reactivity as a New Concept in Organometallic Chemistry. *Acc. Chem. Res.* **2000**, *33*, 139–145.
- (5) Shaik, S.; Hirao, H.; Kumar, D. Reactivity of High-Valent Iron-Oxo Species in Enzymes and Synthetic Reagents: A Tale of Many States. *Acc. Chem. Res.* **2007**, *40*, 532–542.
- (6) Kojima, T.; Hirai, Y.; Ishizuka, T.; Shiota, Y.; Yoshizawa, K.; Ikemura, K.; Ogura, T.; Fukuzumi, S. A Low-Spin Ruthenium(IV)-Oxo Complex: Does the Spin State Have an Impact on the Reactivity? *Angew. Chem., Int. Ed.* **2010**, *49*, 8449–8453.
- (7) Schröder, D.; Shaik, S. Comment on "A Low-Spin Ruthenium-(IV)-Oxo Complex: Does the Spin State Have an Impact on the Reactivity". *Angew. Chem., Int. Ed.* **2011**, *50*, 3850–3851.
- (8) Kojima, T.; Fukuzumi, S. Reply. Angew. Chem., Int. Ed. 2011, 50, 3852–3853.
- (9) Fiedler, A.; Schroeder, D.; Shaik, S.; Schwarz, H. Electronic Structures and Gas-Phase Reactivities of Cationic Late-Transition-Metal Oxides. *J. Am. Chem. Soc.* **1994**, *116*, 10734–10741.
- (10) Yoshizawa, K.; Shiota, Y.; Yamabe, T. Reaction Pathway for the Direct Benzene Hydroxylation by Iron-Oxo Species. *J. Am. Chem. Soc.* **1999**, *121*, 147–153.
- (11) Hirao, H.; Que Jr, L.; Nam, W.; Shaik, S. A Two-State Reactivity Rationale for Counterintuitive Axial Ligand Effects on the C-H Activation Reactivity of Nonheme Fe<sup>IV</sup>=O Oxidants. *Chem. A Eur. J.* **2008**, *14*, 1740–1756.
- (12) Meunier, B.; de Visser, S. P.; Shaik, S. Mechanism of Oxidation Reactions Catalyzed by Cytochrome P450 Enzymes. *Chem. Rev.* **2004**, 104, 3947–3980.
- (13) Hirao, H.; Kumar, D.; Que, L. J.; Shaik, S. Two-State Reactivity in Alkane Hydroxylation by Non-Heme Iron-Oxo Complexes. *J. Am. Chem. Soc.* **2006**, *128*, 8590–8606.
- (14) Abashkin, Y. G.; Collins, J. R.; Burt, S. K. (Salen)Mn(III)-Catalyzed Epoxidation Reaction as a Multichannel Process with Different Spin States. Electronic Tuning of Asymmetric Catalysis: A Theoretical Study. *Inorg. Chem.* **2001**, *40*, 4040–4048.

- (15) Balcells, D.; Raynaud, C.; Crabtree, R. H.; Eisenstein, O. The Rebound Mechanism in Catalytic C-H Oxidation by MnO(Tpp)Cl from DFT Studies: Electronic Nature of the Active Species. *Chem. Commun.* **2008**, 744–746.
- (16) Janardanan, D.; Usharani, D.; Shaik, S. The Origins of Dramatic Axial Ligand Effects: Closed-Shell Mn(V)=O Complexes Use Exchange-Enhanced Open-Shell States to Mediate Efficient H Abstraction Reactions. *Angew. Chem., Int. Ed.* **2012**, *51*, 4421–4425.
- (17) Brandt, P.; Norrby, P. O.; Daly, A. M.; Gilheany, D. G. Chromium Salen-Mediated Alkene Epoxidation: A Theoretical and Experimental Study Indicates the Importance of Spin-Surface Crossing and the Presence of a Discrete Intermediate. *Chem. A Eur. J.* **2002**, *8*, 4299–4307.
- (18) Dhuri, S. N.; Seo, M. S.; Lee, Y.-M.; Hirao, H.; Wang, Y.; Nam, W.; Shaik, S. Experiment and Theory Reveal the Fundamental Difference between Two-State and Single-State Reactivity Patterns in Nonheme Fe(IV)=O versus Ru(IV)=O Oxidants. *Angew. Chem., Int. Ed.* **2008**, 47, 3356–3359.
- (19) Klinker, E. J.; Shaik, S.; Hirao, H.; Que Jr, L. A Two-State Reactivity Model Explains Unusual Kinetic Isotope Effect Patterns in C-H Bond Cleavage by Nonheme Oxoiron(IV) Complexes. *Angew. Chem., Int. Ed.* **2009**, *48*, 1291–1295.
- (20) Dietl, N.; van der Linde, C.; Schlangen, M.; Beyer, M. K.; Schwarz, H. Diatomic [CuO]<sup>+</sup> and Its Role in the Spin-Selective Hydrogen- and Oxygen-Atom Transfers in the Thermal Activation of Methane. *Angew. Chem., Int. Ed.* **2011**, *50*, 4966–4969.
- (21) Abram, S.-L.; Monte-Pérez, I.; Pfaff, F. F.; Farquhar, E. R.; Ray, K. Evidence of Two-State Reactivity in Alkane Hydroxylation by Lewis-Acid Bound Copper-Nitrene Complexes. *Chem. Commun.* **2014**, *50*, 9852–9854.
- (22) Puri, M.; Biswas, A. N.; Fan, R.; Guo, Y.; Que, L. Modeling Non-Heme Iron Halogenases: High-Spin Oxoiron(IV)-Halide Complexes That Halogenate C-H Bonds. *J. Am. Chem. Soc.* **2016**, *138*, 2484–2487.
- (23) Lee, N. Y.; Mandal, D.; Bae, S. H.; Seo, M. S.; Lee, Y.-M.; Shaik, S.; Cho, K.-B.; Nam, W. Structure and Spin State of Nonheme Fe(IV)=O Complexes Depending on Temperature: Predictive Insights from DFT Calculations and Experiments. *Chem. Sci.* **2017**, *8*, 5460–5467.
- (24) Biswas, A. N.; Puri, M.; Meier, K. K.; Oloo, W. N.; Rohde, G. T.; Bominaar, E. L.; Münck, E.; Que Jr, L. Modeling TauD-J: A High-Spin Nonheme Oxoiron (IV) Complex with High Reactivity toward C-H Bonds. J. Am. Chem. Soc. 2015, 137, 2428–2431.
- (25) Bae, S. H.; Seo, M. S.; Lee, Y.-M.; Cho, K.-B.; Kim, W.-S.; Nam, W. Mononuclear Nonheme High-Spin (S = 2) versus Intermediate-Spin (S = 1) Iron(IV)-Oxo Complexes in Oxidation Reactions. *Angew. Chem., Int. Ed.* **2016**, *55*, 8027–8031.
- (26) Xue, G.; De Hont, R.; Münck, E.; Que, L. Million-Fold Activation of the  $[Fe_2(u-O)_2]$  Diamond Core for C-H Bond Cleavage. *Nat. Chem.* **2010**, *2*, 400–405.
- (27) Li, Y.; Handunneththige, S.; Xiong, J.; Guo, Y.; Talipov, M. R.; Wang, D. Opening the  $\operatorname{Co}^{\operatorname{III},\operatorname{IV}}_2(\mu\text{-O})_2$  Diamond Core by Lewis Bases Leads to Enhanced C-H Bond Cleaving Reactivity. *J. Am. Chem. Soc.* **2020**, *142*, 21670–21678.
- (28) Tao, W.; Bower, J. K.; Moore, C. E.; Zhang, S. Dicopper  $\mu$ -Oxo,  $\mu$ -Nitrosyl Complex from the Activation of NO or Nitrite at a Dicopper Center. *J. Am. Chem. Soc.* **2019**, *141*, 10159–10164.
- (29) Tao, W.; Carter, S.; Trevino, R.; Zhang, W.; Shafaat, H. S.; Zhang, S. Reductive NO Coupling at Dicopper Center via a  $[Cu_2(NO)_2]^{2+}$  Diamond-Core Intermediate. *J. Am. Chem. Soc.* **2022**, 144, 22633–22640.
- (30) Tao, W.; Moore, C. E.; Zhang, S. Redox-Neutral S-Nitrosation Mediated by a Dicopper Center. *Angew. Chem., Int. Ed.* **2021**, *60*, 15980–15987.
- (31) Tao, W.; Yerbulekova, A.; Moore, C. E.; Shafaat, H. S.; Zhang, S. Controlling the Direction of S-Nitrosation versus Denitrosation: Reversible Cleavage and Formation of an S-N Bond within a Dicopper Center. *J. Am. Chem. Soc.* **2022**, *144*, 2867–2872.

- (32) Abe, T.; Kametani, Y.; Yoshizawa, K.; Shiota, Y. Mechanistic Insights into the Dicopper-Complex-Catalyzed Hydroxylation of Methane and Benzene Using Nitric Oxide: A DFT Study. *Inorg. Chem.* **2021**, *60*, 4599–4609.
- (33) Skeel, B. A.; Suess, D. L. M. Exploiting Molecular Symmetry to Quantitatively Map the Excited-State Landscape of Iron-Sulfur Clusters. *J. Am. Chem. Soc.* **2023**, *145*, 10376–10395.
- (34) Minkin, V. I.; Starikova, A. A.; Starikov, A. G. Quantum Chemical Modeling of Magnetically Bistable Metal Coordination Compounds. Synchronization of Spin Crossover, Valence Tautomerism and Charge Transfer Induced Spin Transition Mechanisms. *Dalt. Trans.* **2016**, *45*, 12103–12113.
- (35) Bower, J. K.; Sokolov, A. Y.; Zhang, S. Four-Coordinate Copper Halonitrosyl {CuNO}<sup>10</sup> Complexes. *Angew. Chem., Int. Ed.* **2019**, 58, 10225–10229.
- (36) De Buysser, K.; Herman, G. G.; Bruneel, E.; Hoste, S.; Van Driessche, I. Determination of the Number of Unpaired Electrons in Metal-Complexes. A Comparison between the Evans' Method and Susceptometer Results. *Chem. Phys.* **2005**, *315*, 286–292.
- (37) Salomon, O.; Reiher, M.; Hess, B. A. Assertion and Validation of the Performance of the B3LYP Functional for the First Transition Metal Row and the G2 Test Set. *J. Chem. Phys.* **2002**, *117*, 4729–4737.
- (38) Kaltsoyannis, N.; McGrady, J. E.; Harvey, J. N. DFT Computation of Relative Spin-State Energetics of Transition Metal Compounds. *Princ. Appl. Density Funct. Theory Inorg. Chem. I* **2004**, *112*, 151–184.
- (39) Manner, V. W.; Lindsay, A. D.; Mader, E. A.; Harvey, J. N.; Mayer, J. M. Spin-Forbidden Hydrogen Atom Transfer Reactions in a Cobalt Biimidazoline System. *Chem. Sci.* **2012**, *3*, 230–243.
- (40) Angeli, C.; Cimiraglia, R.; Evangelisti, S.; Leininger, T.; Malrieu, J.-P. Introduction of N-Electron Valence States for Multireference Perturbation Theory. *J. Chem. Phys.* **2001**, *114*, 10252–10264.
- (41) Afanasyeva, M. S.; Taraban, M. B.; Purtov, P. A.; Leshina, T. V.; Grissom, C. B. Magnetic Spin Effects in Enzymatic Reactions: Radical Oxidation of NADH by Horseradish Peroxidase. *J. Am. Chem. Soc.* **2006**, *128*, 8651–8658.
- (42) Shaik, S.; de Visser, S. P.; Kumar, D. External Electric Field Will Control the Selectivity of Enzymatic-Like Bond Activations. *J. Am. Chem. Soc.* **2004**, *126*, 11746–11749.
- (43) Herchel, R.; Zoufalý, P.; Nemec, I. The Effect of the Second Coordination Sphere on the Magnetism of [Ln(NO<sub>3</sub>)<sub>3</sub>(H<sub>2</sub>O)<sub>3</sub>]·(18-Crown-6)(Ln= Dy and Er). RSC Adv. **2019**, 9, 569–575.
- (44) Gil, Y.; Llanos, L.; Cancino, P.; Fuentealba, P.; Vega, A.; Spodine, E.; Aravena, D. Effect of Second-Sphere Interactions on the Magnetic Anisotropy of Lanthanide Single-Molecule Magnets: Electrostatic Interactions and Supramolecular Contacts. *J. Phys. Chem. C* 2020, 124, 5308–5320.
- (45) Tao, W.; Bower, J. K.; Moore, C. E.; Zhang, S. Dicopper Moxo, M-nitrosyl Complex from the Activation of NO or Nitrite at a Dicopper Center. *J. Am. Chem. Soc.* **2019**, *141*, 10159–10164.
- (46) Weber, B.; Walker, A. Solution NMR Studies of Iron (II) Spin-Crossover Complexes. *Inorg. Chem.* **2007**, *46*, 190–192.
- (47) Zdilla, M. J.; Dexheimer, J. L.; Abu-Omar, M. M. Hydrogen Atom Transfer Reactions of Imido Manganese(V) Corrole: One Reaction with Two Mechanistic Pathways. *J. Am. Chem. Soc.* **2007**, 129, 11505–11511.
- (48) Lin, Q.; Fu, Y.; Liu, P.; Diao, T. Monovalent Nickel-Mediated Radical Formation: A Concerted Halogen-Atom Dissociation Pathway Determined by Electroanalytical Studies. *J. Am. Chem. Soc.* **2021**, 143, 14196–14206.
- (49) Sandford, C.; Fries, L. R.; Ball, T. E.; Minteer, S. D.; Sigman, M. S. Mechanistic Studies into the Oxidative Addition of Co(I) Complexes: Combining Electroanalytical Techniques with Parameterization. *J. Am. Chem. Soc.* **2019**, *141*, 18877–18889.
- (50) Zhang, C. X.; Liang, H.-C. C.; Kim, E. E. I.; Shearer, J.; Helton, M. E.; Kim, E. E. I.; Kaderli, S.; Incarvito, C. D.; Zuberbühler, A. D.; Rheingold, A. L.; Karlin, K. D. Tuning Copper-Dioxygen Reactivity

- and Exogenous Substrate Oxidations via Alterations in Ligand Electronics. J. Am. Chem. Soc. 2003, 125, 634–635.
- (51) Hatcher, L. Q.; Vance, M. A.; Sarjeant, A. A. N.; Solomon, E. I.; Karlin, K. D. Copper-Dioxygen Adducts and the Side-on Peroxo Dicopper(II)/Bis( $\mu$ -Oxo) Dicopper(III) Equilibrium: Significant Ligand Electronic Effects. *Inorg. Chem.* **2006**, *45*, 3004–3013.
- (52) Maiti, D.; Woertink, J. S.; Sarjeant, A. A. N.; Solomon, E. I.; Karlin, K. D. Copper Dioxygen Adducts: Formation of Bis(μ-Oxo)Dicopper(III) versus (μ-1, 2)Peroxodicopper(II) Complexes with Small Changes in One Pyridyl-Ligand Substituent. *Inorg. Chem.* **2008**, 47, 3787–3800.
- (53) Mandal, D.; Mallick, D.; Shaik, S. Kinetic Isotope Effect Determination Probes the Spin of the Transition State, Its Stereochemistry, and Its Ligand Sphere in Hydrogen Abstraction Reactions of Oxoiron(IV) Complexes. Acc. Chem. Res. 2018, 51, 107–117
- (54) Filatov, M.; Shaik, S. Theoretical Investigation of Two-State-Reactivity Pathways of H-H Activation by FeO<sup>+</sup>: Addition-Elimination, "Rebound", and Oxene-Insertion Mechanisms. *J. Phys. Chem. A* **1998**, *102*, 3835–3846.
- (55) Kwon, Y. H.; Mai, B. K.; Lee, Y. M.; Dhuri, S. N.; Mandal, D.; Cho, K. B.; Kim, Y.; Shaik, S.; Nam, W. Determination of Spin Inversion Probability, H-Tunneling Correction, and Regioselectivity in the Two-State Reactivity of Nonheme Iron(IV)-Oxo Complexes. *J. Phys. Chem. Lett.* **2015**, *6*, 1472–1476.
- (56) Mallick, D.; Shaik, S. Kinetic Isotope Effect Probes the Reactive Spin State, As Well As the Geometric Feature and Constitution of the Transition State during H-Abstraction by Heme Compound II Complexes. J. Am. Chem. Soc. 2017, 139, 11451–11459.
- (57) Truhlar, D. G.; Garrett, B. C. Variational Transition-State Theory. *Annu. Rev. Phys. Chem.* **1984**, 35, 159–189.
- (58) Gao, J. Hybrid Quantum and Molecular Mechanical Simulations: An Alternative Avenue to Solvent Effects in Organic Chemistry. *Acc. Chem. Res.* **1996**, *29*, 298–305.
- (59) Truhlar, D. G.; Garrett, B. C. Variational Transition-State Theory. Acc. Chem. Res. 1980, 235, 440–448.